Phenomenology of ESR in heavy-fermion systems: Fermi-liquid and non-Fermi-liquid regimes

Peter Wölfle[1] and Elihu Abrahams[2]
[1]*Institut für Theorie der Kondensierten Materie, Karlsruhe Institute of Technology (KIT), D-76128 Karlsruhe, Germany*
[2]*Center for Materials Theory, Serin Physics Laboratory, Rutgers University, Piscataway, New Jersey 08854-8019, USA*
(Received 18 September 2009; revised manuscript received 6 November 2009; published 7 December 2009)

We extend and apply a recent theory of the dynamical spin response of Anderson lattice systems to interpret electron-spin resonance (ESR) data on $YbRh_2Si_2$. Starting within a semiphenomenological Fermi-liquid description at low temperatures $T<T_x$ (a crossover temperature) and low magnetic fields $B \ll B_x$, we extend the description to the non-Fermi-liquid regime by adopting a quasiparticle picture with effective mass and spin susceptibility varying logarithmically with energy/temperature as observed in experiment. We find a *sharp* ESR resonance line slightly shifted from the local f-level resonance and broadened by quasiparticle scattering (taking unequal g factors of conduction and f electrons) and by spin-lattice relaxation, both significantly reduced by the effect of ferromagnetic fluctuations. A detailed comparison of our theory with the data shows excellent agreement in the Fermi-liquid regime. In the non-Fermi-liquid regime we find a close relation of the T dependence of the specific-heat/spin susceptibility with the observed T dependence of line shift and linewidth.

DOI: 10.1103/PhysRevB.80.235112 PACS number(s): 71.27.+a, 75.20.Hr, 76.30.−v

I. INTRODUCTION

In several recent experiments,[1,2] low-temperature electron-spin resonance (ESR) has been observed in some heavy-fermion metals, in particular, YRh_2Si_2 (YRS).[1,3,4] The phase diagram of YRS has a magnetic field-induced quantum-critical point and is a model system for the study of quantum criticality in the Kondo lattice. Consequently, the observation of a narrow ESR resonance in this compound aroused great interest, especially since it was commonly believed that heavy-fermion ESR would be unobservable due to an enormous intrinsic linewidth ΔB of order $k_B T_K / g\mu_B$.[1] Here T_K is the lattice coherence (Kondo) temperature for the onset of heavy-fermion behavior and $g\mu_B$ is the gyromagnetic ratio for the resonance. These were the first observations of ESR in Kondo lattice systems at $T<T_K$.

A common feature of the compounds in which ESR has been observed appears to be the existence of ferromagnetic fluctuations[2,5] These findings challenge our understanding of heavy-fermion compounds: how does a sharp electron-spin resonance emerge despite Kondo screening and spin-lattice relaxation and why is this process influenced by ferromagnetic fluctuations? In a recent paper (Ref. 6, referred to as AW in the following) we discussed the background of these questions and answered them in the framework of Fermi-liquid theory. An alternative explanation based on localized spins was subsequently proposed by Schlottmann.[7] The general derivation of Fermi-liquid theory from the microscopic theory for a two-band Anderson lattice model has been given by Yip.[8]

In YRS, the observed narrow Dysonian[9] ESR-line shape was originally interpreted[1] as indicating that the resonance was due to local spins at the Yb sites. Therefore, initially the authors speculated that the narrow ESR line might indicate the suppression of the Kondo effect near the quantum-critical point, since, as explained above, carrying over Kondo impurity physics to the Kondo lattice, one might expect the local spins to be screened by the Kondo effect, giving rise only to a broad spin-excitation peak, too wide to be observed in ESR experiments. However, a closer look[10] revealed that itinerant (heavy) electron ESR could give rise to a similar line shape since the carrier diffusion in YRS is quite slow. Thus, whether the resonance is that of localized or itinerant spins remained an open question.

In this paper, we extend our previous work[6] to the non-Fermi-liquid (NFL) region of the YRS phase diagram and make a detailed comparison with the data. Excellent agreement is obtained for the Fermi-liquid (FL) regime. In particular, the ratio of the contributions $\propto T^2$ and $\propto B^2$ to the linewidth in the FL region is very well reproduced. In addition, we account for the anomalous behavior observed in the NFL region for the resonance line shift and the linewidth, One absolutely essential aspect of our theory is the lattice coherence of the quasiparticles in the Anderson or Kondo lattice model: it is this lattice coherence that is responsible for the absence in the lattice case of the strong local spin relaxation that is observed in single Kondo impurity physics. Attempts to account for the observed logarithmic temperature dependence of the line shift as arising from single Kondo-ion physics above the Kondo temperature are therefore problematic since lattice coherence is lost in that case.

A number of papers[11] have appeared that address the ESR in YRS from the point of view of localized f moments. As we have just discussed, we believe this approach is not appropriate for the experiments in question, which are carried out at temperatures much lower than the observed lattice coherence temperature of about 24 K. Further, the experiments are mostly in or near the region of large Fermi volume; this indicates the importance of the coupling between the f electrons and the conduction electrons and the consequent emergence of heavy quasiparticles, consistent with the starting point of our work.

II. ESR IN THE KONDO-SCREENED ANDERSON LATTICE MODEL: FERMI-LIQUID REGIME

This was analyzed in Sec. III of AW. The Hamiltonian of the simplest Anderson lattice model, assuming momentum-independent hybridization is given by

$$H = \sum_{\mathbf{k},\sigma} \epsilon_{\mathbf{k}\sigma} c^{+}_{\mathbf{k}\sigma} c_{\mathbf{k}\sigma} + \sum_{i,\sigma} \epsilon_{f\sigma} n_{fi\sigma} + U \sum_{i} n_{fi\uparrow} n_{fi\downarrow} + V \sum_{i,\mathbf{k},\sigma} (e^{i\mathbf{k}\cdot\mathbf{R}_i} f^{+}_{i\sigma} c_{\mathbf{k}\sigma} + \text{H.c.}), \quad (1)$$

where $\epsilon_{\mathbf{k}\sigma} = \epsilon_{\mathbf{k}} - \omega_c \sigma/2$, $\sigma = \pm 1$, is the conduction-electron energy spectrum and $\omega_c = g_c \mu_B B$ is its Zeeman splitting; $c^{+}_{\mathbf{k}\sigma}, f^{+}_{i\sigma}$ are creation operators of the conduction electrons in momentum and spin eigenstates $(\mathbf{k}\sigma)$, and of electrons in the local f level at site $\mathbf{R}_i$, respectively. The operator $n_{fi\sigma} = f^{+}_{i\sigma} f_{i\sigma}$ counts the number of electrons on the local level and $\epsilon_{f\sigma} = \epsilon_f - \omega_f \sigma/2$. V and U are the hybridization amplitude and the Coulomb-interaction matrix element. We take the Zeeman splittings ω_c and ω_f to be unequal as they are in real materials.[12] We consider the limit $\omega_f - \omega_c \to 0$ in the Appendix.

We now review the results for the dynamical spin susceptibility $\chi^{+-}(\Omega)$ obtained in AW.[6] We find a single resonance peak

$$\chi^{+-}(\Omega) = \chi^{+-}(0) \frac{-\omega_r + i\Gamma}{\Omega - \omega_r + i\Gamma}, \quad (2)$$

where the resonance frequency is given by[13]

$$\omega_r = \omega_f - \frac{m}{m^*}(\omega_f - \omega_c). \quad (3)$$

Here m^*/m is the quasiparticle effective-mass ratio. We note that for equal g factors the line position is not shifted. In the Appendix, we discuss the complete result, showing that even in the case of unequal g factors there is only a single resonance peak. We also show that the residual Fermi-liquid interaction effects drop out of the resonance frequency.

The linewidth Γ has contributions from quasiparticle scattering and from the conduction-electron spin-lattice relaxation γ

$$\Gamma = A \left[\alpha (\pi T)^2 + \frac{1}{4} (R\omega_f)^2 \right] \frac{1}{R} + 2\gamma \frac{m}{m^*} \frac{1}{R}. \quad (4)$$

Here $R = [1 + \tilde{U}\chi^{+-}(0)]$ is identified as the Wilson ratio, $\tilde{U}$ is the Fermi-liquid spin-exchange interaction,[14] and $\chi^{+-}(0) = M/B$ is the static transverse spin susceptibility (M is the spin polarization). The numerical coefficient α depends on the band structure and is of order unity. In the case of a sizeable ferromagnetic interaction, $(\tilde{U} > 0)$, $R \gg 1$, the linewidth gets narrowed by a factor $1/R$. We suggest that this effect is responsible for the fact that so far an ESR line has only been observed in compounds that exhibit signatures of ferromagnetic fluctuations.

A. Magnetic anisotropy of ESR line

The magnetic response of YRS is strongly anisotropic, largely because of the single-ion anisotropy. The Zeeman Hamiltonian of the f-electron ground-state doublet of Yb in tetragonal symmetry has the form $H_Z = -\mu_B g_{f\perp}(S_x B_x + S_y B_y) - \mu_B g_{f\parallel} S_z B_z$, where the z axis is along the crystallographic c axis. The anisotropy of the g factor is about a factor of 20,

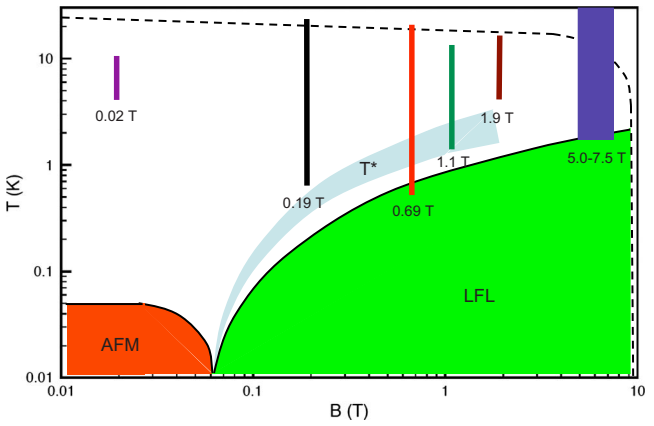

FIG. 1. (Color online) Phase diagram of YRS showing field and temperature ranges of ESR experiments. Magnetic field B in Tesla, temperature T in Kelvin.

$g_{f\perp} = 3.6$ and $g_{f\parallel} = 0.17$. We assume for the present that the anisotropy of the interaction is negligible. The Hamiltonian is then diagonal in the coordinate system in the spin space that diagonalizes H_Z. The eigenvalues of H_Z are found as

$$\omega_f(\phi) = \mp \mu_B B \sqrt{g^2_{f\parallel} \cos^2 \phi + g^2_{f\perp} \sin^2 \phi}, \quad (5)$$

where ϕ is the angle between the magnetic field $\mathbf{B}$ and the c axis.

The above results, Eq. (2), for the dynamical spin susceptibility $\chi^{+-}(\Omega)$ obtained in Ref. 6 for the isotropic model may then be generalized to the anisotropic model by replacing ω_f by $\omega_f(\phi)$ and taking the tensor of spin susceptibility projected onto the direction of the static magnetic field. According to Ref. 15, the angle dependence of the resonance frequency is well represented by Eq. (5). This indicates that the anisotropic part of the residual Fermi-liquid spin-exchange interaction is small. As we shall see later, the temperature dependence of the line shift in the non-Fermi-liquid regime suggests that there may be a small anisotropic interaction component. We shall explore the consequences of such a nonspin-rotation invariant term in Sec. II C, below.

B. ESR-line shift and linewidth in the Fermi-liquid regime

In Fig. 1, we show a sketch of the phase diagram of YRS, including the B, T ranges in which ESR experiments have been carried out. Here, the crossover to the FL regime is determined by the onset of FL behavior in thermodynamic quantities.[16] The T^* crossover is primarily determined by Hall-effect results[17,18] that can be interpreted as a transition (from left to right) to a large Fermi surface.

The high magnetic field ESR data reported in Ref. 3 show a crossover from a low-temperature FL-like regime to a higher temperature non-Fermi-liquid behavior at a temperature $T_x \simeq 5$ K. In the FL regime the line shift appears to be temperature independent. Relative to the ionic g factor of 3.86,[1] the resonance is shifted to lower values on the order of $g_\perp \simeq 3.4-3.45$ independent of magnetic field in the range 5.15–7.45 T (the uncertainty comes mainly from a possible small misalignment of the sample). Estimating the effective-

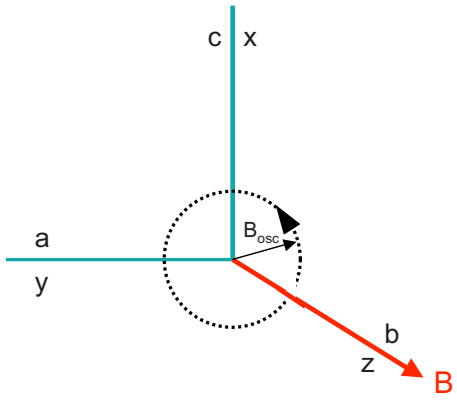

FIG. 2. (Color online) Specification of axes for magnetic fields in ESR experiment.

mass ratio, which is also temperature independent below T_x in the magnetic field range considered, as $m^*/m \sim 40$, we obtain from Eq. (3) a g shift $\Delta g \simeq 0.04$, which is an order of magnitude too small. This discrepancy may point to an additional small anisotropic spin interaction, which we consider in the following section.

As for the linewidth, in the FL regime, Schaufuß, *et al.*[3] find a linewidth that follows the law $\Gamma(T,B) \sim T^2$, extrapolating to $\Gamma(0,B) \sim B^2$ as $T \to 0$. The experimental ratio of the prefactors of the T^2 and B^2 terms, $r_{exp} = B^2[\Gamma(T,B) - \Gamma(0,B)]/[\Gamma(0,B)T^2]$ turns out to be $r_{exp} \sim 2$. Estimating the Wilson ratio from the available specific-heat data[19,20] at $T_x = 5$ K and in magnetic fields $B \approx 6$ T, $\Delta C/T = 0.032$ K^{-1} Yb^{-1} and spin-susceptibility data[20,21] $\Delta\chi = M/B = 0.224\mu_B^2$ K^{-1} Yb^{-1} as $R = [\chi/(g_f\mu_B/2)^2](\pi^2 T/3\Delta C) \simeq 7.5$, we calculate from Eq. (4) the theoretical ratio $r_{th} \sim 1.2\alpha$, in good agreement with the experimental value. Note that the large enhancement of the single-particle Zeeman splitting by the Fermi-liquid interaction (a factor R) is essential in obtaining this agreement. It is worth noting that the anisotropy of the linewidth is weak in the Fermi-liquid regime. Only the B^2 term is strongly anisotropic $\propto \omega_f^2(\phi)$ and thus decreases in magnitude by a factor of ~ 400 when the field orientation changes from perpendicular to parallel to the c axis, which is to say that the B dependence practically disappears for $\mathbf{B} \| \vec{c}$.

C. Effect of nonspin-rotation invariant Fermi-liquid interaction

The spin-orbit interaction in conjunction with the tetragonal lattice anisotropy may be expected to lead to a small admixture of a nonspin-symmetric component to the Fermi-liquid interaction of the form $-4I(\vec{S}\cdot\hat{c})^2$, where $\hat{c}$ is the unit vector along the c axis of the tetragonal lattice. Taking the magnetic field along the b axis, we employ a coordinate system in spin space, in which the z axis is oriented along the magnetic field and the x axis along the c axis (see Fig. 2).

The ESR oscillating transverse magnetic field is circularly polarized in the x-y plane, which is the a-c plane of the crystal, perpendicular to the static magnetic field. The screening of the static magnetic field is affected in linear order in I only when the component of the magnetic field along $\hat{c}$ is nonvanishing. In turn, the dynamic screening is changed at linear order in I, for any component of $\mathbf{B}_{static}$ perpendicular to $\hat{c}$. Thus, the static and dynamic screenings are effected differently by I, which gives rise to a resonance line shift, which we now calculate. As we show in the Appendix, the dynamical screening of the ff component of the dynamical susceptibility is modified in the presence of I to

$$\chi_{ff}^{+-}(i\Omega_m) = \chi_{ff,H}^{+-}(i\Omega_m)[1 + \tilde{U}_d\chi_{ff}^{+-}(i\Omega_m)].$$

Thus, in the transverse spin response, the Fermi-liquid interaction is changed to $\tilde{U}_d = \tilde{U} + I\sin^2\phi$. The notation is as in AW,[6] Eqs. (16)–(18): $\chi_{ff,H}$ is the susceptibility of Fermi-liquid quasiparticles in the absence of vertex corrections (bubble diagram only) and the subscript H indicates that the bare Zeeman energy ω_f is replaced everywhere by

$$\tilde{\omega}_f = \omega_f[1 + \tilde{U}_s\chi_{ff}^{+-}(0)] = \omega_f[1 - \tilde{U}_s\chi_{ff,H}^{+-}(0)]^{-1}.$$

Here $\tilde{U}_s = \tilde{U} + 4I\cos^2\phi$ and $\tilde{U}$ is the renormalized onsite ff repulsion that appears in the effective low-energy Hamiltonian (see AW for further details). The resonance position is therefore shifted as

$$\omega_r = \tilde{\omega}_{\mathbf{k}_F}^-[1 - \tilde{U}_d\chi_{ff,H}^{+-}(0)] = \omega_{k_F}^- \frac{1 - \tilde{U}_d\chi_{ff,H}^{+-}(0)}{1 - \tilde{U}_s\chi_{ff,H}^{+-}(0)}.$$

Substituting $\omega_{k_F}^-$ as obtained in the Appendix and using the definition of R, we find that the resonance frequency is modified from Eq. (3) to

$$\begin{aligned}\omega_r &\simeq \omega_{k_F}^-[1 - I\chi_{ff,H}^{+-}(0)R] \\ &\simeq \omega_f - \frac{m}{m^*}(\omega_f - \omega_c) \\ &\quad - \omega_f I(1 - 5\cos^2\phi)\chi_{ff}^{+-}(0)\end{aligned}$$

or

$$g_r \simeq g_f - \frac{m}{m^*}(g_f - g_c) - g_f I(1 - 5\cos^2\phi)\chi_{ff}^{+-}(0). \quad (6)$$

Since most of the ESR data have been taken in the configuration of magnetic field perpendicular to the c axis, i.e. $\phi = \pi/2$, we concentrate on this case from now on. We may try to determine I by fitting the low-temperature line shift.[3] In the following, we assume I to be independent of temperature and magnetic field. In the NFL regime, experimentally $\chi_{ff}^{+-}(0;T)$ is a decreasing function of temperature, such that the g shift increases as observed in experiment, provided $I > 0$. We may relate I to $\chi_{ff}^{+-}(0;T_1)$ at a reference point $T_1 = 4$ K, $B = 0.2$ T, where $\chi_{ff}^{+-}(0;T_1) \approx 1.3 \times 10^{-6}$ m^3/mol (Ref. 22) as $I = (g_f^{ion} - g_r)/(g_f\chi_{ff}^{+-})$ [the reference g factor g_f^{ion} is actually reduced by the factor $(1 - m/m^*)$]. The data at low magnetic fields, $B = 0.18$ T and $B = 0.68$ T show a g factor of $g \simeq 3.5$ at the lowest temperature, $T = 2$ K, whereas the high-field data show $g = 3.4 - 3.45$ in the Fermi-liquid regime. It follows that $I \approx 0.075 \times 10^6$ m^{-3} mol. From a comparison with the temperature dependence of the resonance frequency we determine in the next section a value of $I = 0.063$

TABLE I. Experimental values of susceptibility and specific-heat coefficient and calculated g shift [from Eq. (6)] at different B and two temperatures $T_1=4$ K and $T_2=10$ K. We chose $I=0.063\times10^6$ mol/m^3. Units: χ in 10^{-6} m^3/mol, γ in J/(molK^2).

B(T)	$\chi(T_1)$	$\chi(T_2)$	$\gamma(T_1)$	$\gamma(T_2)$	$\delta g(T_1)$	$\delta g(T_2)$	$\frac{\Delta g}{\Delta \ln T)_{th}}$
7.5	0.82	0.65	0.24	0.185	−0.222	−0.197	0.027
6.0	0.91	0.70	0.26	0.18	−0.239	−0.210	0.032
5.0	0.98	0.74	0.27	0.17	−0.254	−0.222	0.035
1.85	1.13	0.78	0.29	0.15	−0.283	−0.238	0.050
1.0	1.2	0.80	0.29	0.15	−0.298	−0.243	0.060
0.68	1.23	0.80	0.29	0.15	−0.305	−0.243	0.068
0.5	1.25	0.80	0.29	0.15	−0.309	−0.243	0.072
0.2	1.3	0.80	0.29	0.15	−0.320	−0.243	0.085

$\times10^6$ m^{-3} mol, which agrees very well with the independently obtained value above. We observe in passing that the magnetic-susceptibility data indicate that in the non-Fermi-liquid regime $\tilde{U}$ appears to depend on both temperature and magnetic field.

III. ESR IN THE NON-FERMI-LIQUID REGIME

We now attempt to phenomenologically relate the framework we have set up to the ESR data in the NFL regime by using the observed specific heat and susceptibility T and B dependences. The non-Fermi-liquid behavior in the temperature range $T>T_x$ appears in the ESR data as a nearly logarithmic increase in the g factor with temperature and a change in the temperature dependence of the linewidth from T^2 to T. This change into the NFL regime occurs at about the same temperature as the observed changes in the specific heat and spin susceptibility.

A. Resonance shift

In the theoretical resonance shift, Eq. (6), the T and B dependences enter in two ways, if we continue to assume that the temperature dependence of the anisotropic Fermi-liquid interaction parameter I may be neglected: (1) through the susceptibility $\chi^{+-}_{ff}(0)$, which we get from experiment and (2) through the effective-mass ratio, which we extract from the measured specific-heat γ coefficient ($\Delta C=\gamma T$), by taking $\gamma\propto m^*/m$. Using these experimentally determined quantities, we shall use Eq. (6) to evaluate the theoretical resonance shift and compare it to the observed one.

We shall use Eq. (6) to calculate the g shift $\delta g=g-g_f^{ion}$ at two reference temperatures $T=4$ K and $T=10$ K. The inputs are the values of m/m^* from the observed specific heat,[19] taking $m^*/m=40$ at $T=5$ K and $B=6$ T as a reference point, the observed susceptibility[21,22] and the value of the anisotropic FL interaction I. These data and the calculated g shifts are collected in Table I. Since we have assumed that I is independent of T and B, we can evaluate it from Eq. (6) using experimental data at $T=4$ K and $B=0.2$ T as discussed in the previous section. The result is $I=0.063\times10^6$ mol/m^3 The data on the ESR-line shift given in Fig. 2 of Ref. 3 show an approximately linear ln T dependence in the T range 4 K$<T<$10 K. Therefore, to check the accuracy of our theoretical result, Eq. (6), we fit the two calculated δg values to a linear ln T function and give the resulting theoretical slope in the last column of Table I. The comparison of the calculated and observed values of the slope $\Delta g/\Delta \ln T$ is shown in Fig. 3. It is seen that the agreement is quite good, supporting our assumption of a constant interaction I. The theory explains the rather strong dependence of the ln T term on magnetic field, decreasing by approximately a factor of 8 as the magnetic field is stepped up from 0.19 to 7.45 T. The present theory predicts that the slope of the ln T dependence of the g shift depends sensitively on the magnetic field orientation (the angle ϕ) and it reverses sign when $\mathbf{B}_{static}$ is oriented along the $\hat{c}$ axis of the crystal.

B. Linewidth

Turning now to the linewidth, we use the analyticity properties of the self-energy $\Sigma(\omega)$ to infer the linewidth from the temperature dependence of the specific-heat coefficient $\gamma(T)$. Here one has to observe that only part of the specific-heat enhancement is coming from the nonanalytic contribution of the self-energy Σ. An additional part is coming from the regular (analytic) contribution to Σ. Therefore one may split

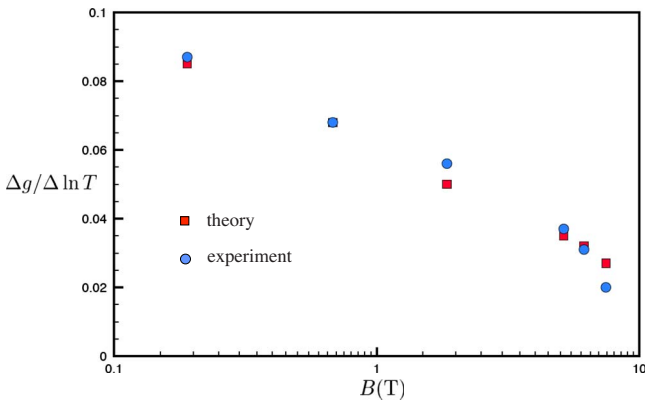

FIG. 3. (Color online) Comparison of g-shift slopes for different B. The theoretical and experimental values are identical at $B=0.68$ T. Specific heat c in J/(mol K).

the effective mass into two components, $m^*/m=(m^*/m)_{reg}+(m^*/m)_{sing}$. The specific-heat data show a $\ln T$ variation over a wide range on top of a background. If we identify the background with $(m^*/m)_{reg}$, the singular part at the reference point $T=5$ K and $B=6$ T is about 60% of the total, i.e., $(m^*/m)_s=24$, taking the FL value $m^*/m=40$. The singular part can now be associated with the non-Fermi-liquid logarithmic temperature dependence of γ. Thus, $\gamma_{sing} \propto (m^*/m)_{sing}$. To account for the crossover from NFL to FL behavior at $T=T_x$, we adopt an interpolation formula $\gamma_{sing}=-c\ln[(T^2+T_x^2)/T_0^2]$. Since $(m^*/m)=[1-\mathrm{Re}\{\partial\Sigma/\partial\omega\}|_0]$, we may write $(m^*/m)_{sing}=-\mathrm{Re}\{\partial\Sigma_{sing}/\partial\omega\}|_0$. The temperature dependence $(m^*/m)_{sing}=-a\ln[(T^2+T_x^2)/T_0^2]$ may be approximately converted into a frequency dependence $\mathrm{Re}\{\partial\Sigma_{sing}/\partial\omega\}=a\ln[(\omega^2+T_x^2)/T_0^2]$ of the nonanalytic real part of the self-energy. The self-energy in the complex plane may be inferred as

$$\Sigma_{sing}(\omega)=2a\omega\ln[(-i\omega+T_x)/T_0].$$

From this approximate model the imaginary part of the self-energy and hence the quasiparticle contribution [the first term in Eq. (4)] to the ESR-line width follows as

$$\Gamma_{qp}=2\frac{m}{m^*}\frac{1}{R}\mathrm{Im}\,\Sigma_s(\omega=T)=pT\tan^{-1}(T/T_x).$$

In the limit of $T\ll T_x$ the above expression recovers the Fermi-liquid result $\Gamma_{qp}\propto T^2$ as discussed above while at $T\gg T_x$ the non-Fermi-liquid result $\Gamma_{qp}\propto T$ is obtained. This is in qualitative agreement with experiment. It is worth pointing out that a similar structure of the self-energy has been proposed for the "strange-metal" phase of the cuprates under the name "marginal Fermi-liquid theory."[23] By comparison with the effective-mass ratio we find $a_{th}\approx 6$ and using $R\approx 7$ we get $p_{th}\approx 0.1$. The experimental value is $p_{ex1}\approx 0.02$, which is quite a bit smaller. Similarly, from the experimentally observed coefficient of the T^2 term of the linewidth, $\Gamma/T^2\approx 0.004$ K^{-1} in the Fermi-liquid regime, one extracts again a value $p_{ex2}\approx 0.02$. The discrepancy may come from our assumption that Σ_{sing} is entirely due to spin-flip scattering and from our very approximate determination of Σ_{sing}. Vertex corrections will, for example, remove any nonspin interaction contribution to Σ_{sing} from the linewidth Γ. If this is correct, it would imply that the fluctuations contributing most to the $\ln T$ term in the specific heat are nonmagnetic in origin. Finally we comment on the possible contribution to Γ caused by the regular part of $\Sigma_{reg}(\omega)$. In this case the prefactors c_r, c_i of the low-energy limiting forms $\mathrm{Re}\,\Sigma_{reg}(\omega)=\Sigma_{reg}(0)+c_r\omega$ and $\mathrm{Im}\,\Sigma_{reg}(\omega)=c_i\omega^2$ are not directly related. The Kramers-Kronig relations imply in this case that, e.g., the higher frequency parts of $\mathrm{Re}\,\Sigma_{reg}(\omega)$ will predominantly determine the coefficient c_i while the coefficient c_r has little influence in this. In the present case, the resulting imaginary part and coefficient c_i is apparently small.

IV. CONCLUSION

We extended and applied our recent theory[6] of the dynamical spin response of Anderson lattice systems to interpret ESR data on $YbRh_2Si_2$. Starting with a semiphenomenological Fermi-liquid description at low temperatures $T<T_x$ (a crossover temperature) and low magnetic fields $B\ll B_x$, we extended the description to the non-Fermi-liquid regime by adopting a quasiparticle picture with effective mass and spin susceptibility varying logarithmically with energy/temperature as observed in experiments. We find a *sharp* ESR resonance line that is broadened by quasiparticle scattering and spin-lattice relaxation, both significantly reduced by the effect of ferromagnetic fluctuations. A more complete evaluation of the results presented in our first paper shows that the ESR-line position is shifted by an amount $\propto(g_f-g_c)$, thus reducing to zero for equal g factors. In the case of different g factors there is only one sharp resonance line at $\omega\simeq\omega_f$, the local f-resonance frequency. The observed strong anisotropy of the ESR response is shown to follow from the single-ion spin anisotropy, assuming an approximately spin-conserving exchange interaction.

A detailed comparison of our theory with the data shows excellent agreement in the Fermi-liquid regime, when the model is amended by a small anisotropic part of the spin-exchange interaction, induced by spin-orbit coupling. We assumed the strength of the latter to be independent of temperature and magnetic field throughout the regime considered in the experiments. In particular, the ratio of the contributions $\propto T^2$ and $\propto B^2$ to the linewidth in the FL region is very well reproduced by theory.

In the non-Fermi-liquid regime we find a close relation of the T dependences of the specific heat and spin susceptibility with the observed T dependences of the line shift and linewidth. There are two terms contributing to the temperature dependence of the lineshift [Eq. (6)] in opposite ways. The first and dominant one is proportional to the spin susceptibility χ and leads to a resonance frequency increasing with temperature while the second and smaller one is proportional to the inverse specific-heat coefficient $1/\gamma$, leading to a decreasing behavior. The observed approximately linear in $\ln T$ dependence of the g shift is determined by χ and $1/\gamma$, (in the restricted temperature regime, where the remaining curvature in both χ and $1/\gamma$ tends to compensate) while the magnitude of the shift is fitted by adjusting the anisotropic exchange-interaction constant I. The observed rather strong magnetic field dependence of the prefactor of $\ln T$ is very well accounted for by χ. Finally, we attempted to relate the linewidth to the singular part of the self-energy Σ_{sing}, by identifying the $\ln T$ contribution to the specific heat coefficient with the effective mass deduced from Σ_{sing}. On a qualitative level, the observed crossover from T^2 to linear T behavior of the linewidth upon entering the non-Fermi-liquid regime is reproduced. However, the line width is found to be approximately a factor of 5 too large compared to experiment. The most likely explanation of this discrepancy is our neglect of vertex corrections, which would remove any nonmagnetic contribution to Σ_{sing} from the linewidth.

The recent observation of Duque *et al.*[4] that there is a dramatic suppression of the ESR signal when the nonmagnetic Lu dopants on Yb sites in YRS exceed 15% is consistent with our picture: it implies that the lattice coherence that is essential for the observation of a narrow ESR line breaks down for doping beyond 15%. Overall the extended quasi-

particle picture used to account for the ESR properties in the non-Fermi-liquid regime appears to work quite well. It would be interesting to compare with data taken at much lower temperatures, when the present theory would predict, e.g., nonlinear variation in the g shift with $\ln T$ as exhibited by χ. Also, a cleaner identification of the linear T dependence of the linewidth would be essential to corroborate the extended quasiparticle picture. Finally, our theory makes definite predictions for the anisotropy of the line shift.

ACKNOWLEDGMENTS

We are grateful to J. Sichelschmidt and his colleagues for several extensive discussions of their work. Helpful comments by V. Kataev are acknowledged. We thank the Aspen Center for Physics, where part of this work was completed. P.W. acknowledges partial support from the DFG—Center for Functional Nanostructures and the DFG—Forschergruppe "Quantum Phase Transitions."

APPENDIX

1. Derivation of dynamical susceptibility: spin-rotation invariant Fermi-liquid interaction

In this appendix we derive the quasiparticle properties and the dynamical spin susceptibility in a more detailed and complete way than was done in AW.[6] We start from the Dyson equation for the single-particle Green's functions

$$\mathcal{G}^{-1}\mathcal{G} = \begin{bmatrix} i\omega_n - \epsilon_{f\sigma} - \Sigma_{f\sigma}(i\omega_n,\mathbf{k}) & -V \\ -V & i\omega_n - \epsilon_{\mathbf{k}\sigma} - \Sigma_{c\sigma}(i\omega_n,\mathbf{k}) \end{bmatrix} \times \begin{pmatrix} G^{ff}_{\mathbf{k}\sigma} & G^{cf}_{\mathbf{k}\sigma} \\ G^{fc}_{\mathbf{k}\sigma} & G^{cc}_{\mathbf{k}\sigma} \end{pmatrix} = 1. \tag{A1}$$

We approximate the conduction-electron retarded self-energy by $\Sigma_{c\sigma}(\omega+i0,\mathbf{k})=-i\gamma$, where γ is the conduction-electron spin-lattice relaxation rate. To carefully derive the quasiparticle Zeeman energies, we make use of the conservation of total spin in the model considered here, to remove the f-electron Zeeman term of the Hamiltonian by performing a gauge transformation that shifts the zero of energy of $\uparrow$ spins and $\downarrow$ spins by $\mp\omega_f/2$, respectively. As a consequence $i\omega_n$ is replaced by $i\omega_n+\sigma\omega_f/2$, $\epsilon_{f\sigma}$ by ϵ_f and the conduction-electron Zeeman energy is changed to $-\sigma(\omega_f-\omega_c)/2$. For an isotropic band structure ($\epsilon_{\mathbf{k}}=\epsilon_k$), the magnetic field dependence of the self-energy (neglecting small band-edge terms) is then of the form

$$\Sigma_{f\sigma}(\omega+i0,\mathbf{k}) \simeq \Sigma_f[\omega+\sigma\omega_f/2+i0,\epsilon_k-\sigma(\omega_f-\omega_c)/2].$$

In $\mathcal{G}^{-1}_{11}$, we expand this f self-energy about the Fermi energy

$$\begin{aligned}\omega+\sigma\omega_f/2-\epsilon_f-\Sigma_{f\sigma}(\omega+i0,\mathbf{k}) &= (\omega+\sigma\omega_f/2)(1-\partial\Sigma_f/\partial\omega|_0)-\epsilon_f-\Sigma_f(i0,\epsilon_{k_F}) \\ &\quad -(\partial\Sigma_f/\partial\epsilon_k|_{k_F})[\epsilon_k-\epsilon_{k_F}-\sigma(\omega_f-\omega_c)/2] \\ &\quad +i\,\mathrm{Im}\,\Sigma_f(\omega+i0,\epsilon_k) \\ &= z^{-1}[\omega-\tilde{\epsilon}_{fk\sigma}+i\gamma_{fk}],\end{aligned} \tag{A2}$$

where

$$z^{-1} = 1-\partial\Sigma_f/\partial\omega|_0,$$

$$\tilde{\epsilon}_{fk\sigma} = \tilde{\epsilon}_{fk}-\sigma\omega_f/2+\sigma(\partial\Sigma_f/\partial\epsilon_k|_{k_F})(\omega_f-\omega_c)/2,$$

$$\tilde{\epsilon}_{fk} = z[\epsilon_f+\Sigma_f(i0,\epsilon_{k_F})+(\partial\Sigma_f/\partial\epsilon_k|_{k_F})(\epsilon_k-\epsilon_{k_F})],$$

and

$$\gamma_{fk} = z\,\mathrm{Im}\,\Sigma_f(\omega+i0,\epsilon_k).$$

Then for low energies one has a quasiparticle description with $G^{ff}_{\mathbf{k}\sigma}(\omega)=z_\sigma\tilde{G}^{ff}_{\mathbf{k}\sigma}$, $G^{cf}_{\mathbf{k}\sigma}=\sqrt{z_\sigma}\tilde{G}^{cf}_{\mathbf{k}\sigma}$, and the renormalized hybridization amplitude $\tilde{V}^2=z_\sigma V^2$. The complex-energy eigenvalues are given by

$$\begin{aligned}\zeta^{\pm}_{\mathbf{k}\sigma} &= \frac{1}{2}(\tilde{\epsilon}_{f\sigma}-i\gamma_{fk}+\epsilon_{\mathbf{k}\sigma}-i\gamma) \\ &\quad \pm\sqrt{\frac{1}{4}(\tilde{\epsilon}_{f\sigma}-i\gamma_{fk}-\epsilon_{\mathbf{k}\sigma}+i\gamma)^2+\tilde{V}^2} \\ &= \epsilon^{\pm}_{\mathbf{k}}-\frac{1}{2}\sigma\omega^{\pm}_{\mathbf{k}}-i\gamma^{\pm}_{\mathbf{k}},\end{aligned} \tag{A3}$$

where, assuming $|\epsilon_{\mathbf{k}_F}|\gg|\tilde{\epsilon}_{fk}|,\tilde{V}$

$$\epsilon^{\pm}_{\mathbf{k}} = \epsilon^{\pm}_{k_F}+\frac{1}{2}(\epsilon_k-\epsilon_{k_F})(1+z(\partial\Sigma_f/\partial\epsilon_k|_{k_F}))\times\left[1\pm\frac{\epsilon_{\mathbf{k}_F}-\tilde{\epsilon}_f}{\sqrt{(\tilde{\epsilon}_f-\epsilon_{\mathbf{k}_F})^2+4\tilde{V}^2}}\right],$$

$$\omega^{\pm}_{\mathbf{k}} = \omega_f+\frac{1}{2}[(\omega_c-\omega_f)(1+z(\partial\Sigma_f/\partial\epsilon_k|_{k_F}))\times\left[1\pm\frac{\epsilon_{\mathbf{k}_F}-\tilde{\epsilon}_f}{\sqrt{(\tilde{\epsilon}_f-\epsilon_{\mathbf{k}_F})^2+4\tilde{V}^2}}\right],$$

$$\gamma^{\pm}_{\mathbf{k}\sigma} = \frac{1}{2}(\gamma_{fk}+\gamma)\mp\frac{1}{2}(\gamma_{fk}-\gamma)\frac{\epsilon_{\mathbf{k}\sigma}-\tilde{\epsilon}_{f\sigma}}{\sqrt{(\tilde{\epsilon}_f-\epsilon_{\mathbf{k}_F})^2+4\tilde{V}^2}}. \tag{A4}$$

From now on we can safely neglect the term involving $(\partial\Sigma_f/\partial\epsilon_k|_{k_F})$ since it is small—of order $z\ll 1$. Using partial fraction decomposition, we construct the retarded Green's function

$$\tilde{G}^{ff}_{\mathbf{k}\sigma}(\omega+i0) = \frac{a^{ff,+}_{\mathbf{k}\sigma}}{\omega-\zeta^{+}_{\mathbf{k}\sigma}}+\frac{a^{ff,-}_{\mathbf{k}\sigma}}{\omega-\zeta^{-}_{\mathbf{k}\sigma}} \tag{A5}$$

and similar expressions for $\tilde{G}^{cf}_{\mathbf{k}\sigma}$ and $G^{cc}_{\mathbf{k}\sigma}$, where, with $u_{\mathbf{k}\sigma}=\zeta^{+}_{\mathbf{k}\sigma}-\zeta^{-}_{\mathbf{k}\sigma}$

$$a^{ff,\pm}_{\mathbf{k}\sigma} = \pm(\zeta^{\pm}_{\mathbf{k}\sigma}-\tilde{\epsilon}_{\mathbf{k}\sigma})/u_{\mathbf{k}\sigma},$$

$$a_{\mathbf{k}\sigma}^{cc,\pm} = \pm (\zeta_{\mathbf{k}\sigma}^{\pm} - \epsilon_{f\sigma})/u_{\mathbf{k}\sigma},$$

$$a_{\mathbf{k}\sigma}^{cf,\pm} = \pm \tilde{V}/u_{\mathbf{k}\sigma}.$$

For sufficiently small imaginary parts, $\gamma \ll (\tilde{V}, \tilde{\epsilon}_{f\sigma})$, we may neglect them in the weight factors $a_{\mathbf{k}\sigma}^{ff,\pm}, \ldots$ and replace $\zeta_{\mathbf{k}\sigma}^{\pm}$ by $\epsilon_{\mathbf{k}\sigma}^{\pm}$. The quasiparticles interact via the residual Fermi-liquid interaction. For ESR, the relevant component of the Fermi-liquid interaction is the spatially isotropic spin-antisymmetric part described by the Landau parameter $F_0^a = -2N_0\tilde{U}$. Here $\tilde{U}$ is the coupling constant of a spin isotropic exchange interaction $H_{ex} = -\tilde{U}\vec{S}\cdot\vec{S}$, which leads to a quasiparticle energy shift $\delta\omega_{\mathbf{k}} = \tilde{U}M$, where the spin polarization M is given by $M = \chi_H \tilde{\omega}_{k_F}$, with χ_H as the unscreened static spin susceptibility (in the absence of the Fermi-liquid interaction) and $\tilde{\omega}_{k_F}$ the fully renormalized quasiparticle Zeeman splitting at the Fermi energy.

For definiteness in the following we assume a band filling of somewhat less than two electrons per site, such that the Fermi level lies in the lower quasiparticle band (energy $\zeta_{\mathbf{k}\sigma}^{\pm}$) and $\tilde{\epsilon}_{f\sigma}$ is close to the Fermi energy. The screened Zeeman splitting is then obtained by solving the self-consistent equation $\tilde{\omega}_{k_F} = \omega_{k_F}^{-} + \tilde{U}\chi_H\tilde{\omega}_{k_F}$. The solution is

$$\tilde{\omega}_{k_F} = \frac{\omega_{k_F}^{-}}{1 - \tilde{U}\chi_H} = \omega_{k_F}^{-} R, \tag{A6}$$

where $R = 1/(1 - \tilde{U}\chi_H)$ is the Wilson ratio. One observes that in the case of ferromagnetic correlations, when $R \gg 1$, the single-particle Zeeman splitting is enhanced by a large factor. We conjecture that this effect should be observable in tunneling experiments. In the two-particle spectrum probed by electron-spin resonance, the enhancement is completely removed by dynamical screening (see AW).

As derived in AW, the dynamical transverse susceptibility $\chi^{+-}(\Omega)$, where Ω is the frequency of an ac electromagnetic-field-polarized transverse to the static magnetic field, is given by

$$\chi^{+-}(\Omega) = \mu_B^2[g_c^2\chi_{cc}^{+-}(\Omega) + g_f^2\chi_{ff}^{+-}(\Omega) + 2g_c g_f \chi_{cf}^{+-}(\Omega)].$$

The partial susceptibilities are obtained by evaluating Feynman bubble diagrams dressed by vertex corrections of the ladder type referring to the Fermi-liquid interaction (local electrons) and the spin-orbit interaction (impurity correlation lines for the conduction electrons). The final result obtained in AW may be reexpressed as

$$\chi^{+-}(\Omega + i0) = \mu_B^2 \left\{ \{[g_f\chi_{ff}^{+-}(0) + g_c\chi_{cf}^{+-}(0)]^2/\chi_{ff}^{+-}(0)\} \frac{-\omega_r + i\Gamma}{\Omega - \omega_r + i\Gamma} + g_c^2 \frac{-\omega_{\mathbf{k}_F}^{-} + 2i\gamma_{\mathbf{k}_F}^{-}}{\Omega - \omega_{\mathbf{k}_F}^{-} + 2i\gamma_{\mathbf{k}_F}^{-}} \{\chi_{cc,H}^{+-}(0) - [\chi_{cf,H}^{+-}(0)]^2/\chi_{ff,H}^{+-}(0)\} \right\}$$

There appear to be two different resonance denominators in the above expression. Only the resonance at ω_r has been observed in ESR experiments The resonance at $\omega_{\mathbf{k}_F}^{-}$, is shifted to much higher frequencies (the factor R)! However, a closer look reveals that the weight of the resonance at $\omega_{\mathbf{k}_F}^{-}$ is zero in the regime considered. Indeed, by inserting the quasiparticle weight factors, $\chi_{ab,H}^{+-}(0) \simeq 2N_0(a_{\mathbf{k}_F\sigma}^{ab,-})^2$, where a,b is c or f, one finds that the prefactor of the second resonance is zero. In the limit of equal g factors, the prefactor of the first resonance simplifies to $2N_0R$ and its position is unshifted, $\omega_r = \omega_f$. In the absence of spin-lattice relaxation, the linewidth shrinks to zero in this case. This is not reproduced in the above calculation since we did not take into account the vertex corrections belonging to the imaginary part of the self-energy (the scattering-in term in Boltzmann equation language).

2. Non-spin-rotation invariant Fermi-liquid interaction

The relatively large g shift observed in experiment suggests the presence of a small additional spin-symmetry-breaking Fermi-liquid interaction $\mathbf{I}$. Since this interaction can only be mediated by the spin-orbit interaction it should have preferred direction given by the lattice symmetry. We therefore assume the form $\mathbf{I}_{\alpha\beta;\gamma\delta} = -I(\mathbf{c}\cdot\boldsymbol{\tau}_{\alpha\beta})(\mathbf{c}\cdot\boldsymbol{\tau}_{\gamma\delta})$, where $\boldsymbol{\tau}$ is the vector of Pauli matrices and $\mathbf{c}$ is a unit vector in the direction of the crystallographic c axis of the tetragonal lattice. The screened and unscreened tensor susceptibilities $\mathbf{X}, \mathbf{X}_H$, where $\mathbf{X}_{ij} = \langle\langle S_i; S_j\rangle\rangle$, $i = x,y,z$, are connected by the Bethe-Salpeter equation

$$\mathbf{X} = \mathbf{X}_H + \tilde{U}(\mathbf{X}_H\mathbf{X}) + 4I(\mathbf{X}_H\cdot\mathbf{c})(\mathbf{c}\cdot\mathbf{X}).$$

The solution is given by

$$\mathbf{X} = (1 - \tilde{U}\mathbf{X}_p)^{-1}\mathbf{X}_p,$$

where $\mathbf{X}_p$ is the projected unscreened susceptibility

$$\mathbf{X}_p = \mathbf{X}_H + \frac{4I}{1 - 4I\chi_H^{cc}}(\mathbf{X}_H\cdot\mathbf{c})(\mathbf{c}\cdot\mathbf{X}_H), \quad \chi_H^{cc} = (\mathbf{c}\cdot\mathbf{X}_H\cdot\mathbf{c}).$$

To linear order in I the general expression simplifies to

$$\mathbf{X} = [1 - \tilde{U}\mathbf{X}_H - 4I\mathbf{X}_H^{-1}(\mathbf{X}_H\cdot\mathbf{c})(\mathbf{c}\cdot\mathbf{X}_H)]^{-1}\mathbf{X}_H.$$

In the main configuration of the experiments, the static magnetic field is oriented parallel to the ab plane, say along the a axis. We take this to be the z axis in spin space and identify the c axis with the x axis. Then we see that the screening of the static field is not changed to linear order in I, as $\mathbf{X}_{+z} = \mathbf{X}_{z+} = 0$, etc. The dynamical response with the time-dependent magnetic field oriented perpendicular to the z axis is, however modified. Using $\chi^{+x}\chi^{x-} = \frac{1}{4}(\chi^{+-})^2$ we find

$$\chi^{+-} = \chi_H^{+-}/[1 - (\tilde{U} + I)\chi_H^{+-}].$$

[1] J. Sichelschmidt, V. A. Ivanshin, J. Ferstl, C. Geibel, and F. Steglich, Phys. Rev. Lett. **91**, 156401 (2003).
[2] C. Krellner, T. Forster, H. Jeevan, C. Geibel, and J. Sichelschmidt, Phys. Rev. Lett. **100**, 066401 (2008).
[3] U. Schaufuß, V. Kataev, A. A. Zvyagin, B. Büchner, J. Sichelschmidt, J. Wykhoff, C. Krellner, C. Geibel, and F. Steglich, Phys. Rev. Lett. **102**, 076405 (2009).
[4] J. G. S. Duque, E. M. Bittar, C. Adriano, C. Giles, L. M. Holanda, R. Lora-Serrano, P. G. Pagliuoso, C. Rettori, C. A. Pérez, Rongwei Hu, C. Petrovic, S. Maquilon, Z. Fisk, D. L. Huber, and S. B. Oseroff, Phys. Rev. B **79**, 035122 (2009).
[5] P. Gegenwart, J. Custers, Y. Tokiwa, C. Geibel, and F. Steglich, Phys. Rev. Lett. **94**, 076402 (2005).
[6] E. Abrahams and P. Wölfle, Phys. Rev. B **78**, 104423 (2008).
[7] P. Schlottmann, Phys. Rev. B **79**, 045104 (2009).
[8] S.-K. Yip, Phys. Rev. B **38**, 8785 (1988).
[9] G. Feher and A. F. Kip, Phys. Rev. **98**, 337 (1955).
[10] E. Abrahams (unpublished).
[11] e.g., D. L. Huber, J. Phys.: Condens. Matter **21**, 322203 (2009). In this work, the *g*-factor anisotropy for the localized spin model was considered.
[12] In YRS there is a crystal-field doublet ground state of the Yb^{3+} ion, which is treated as a pseudospin 1/2 in our model. This is justified since the splitting to the next higher multiplet is much larger ($\approx$120 K) that the temperature of the experiments. Therefore the issue of the (pseudo)spin conservation or not in the Anderson lattice model does not arise.
[13] The term proportional to m/m^* was inadvertently misevaluated in Eq. (20) of AW.
[14] In the familiar Fermi-liquid notation, $F_0^a = -2N_0\tilde{U}$.
[15] J. Sichelschmidt, J. Wykhoff, H.-A. Krug von Nidda, J. Ferstl, C. Geibel, and F. Steglich, J. Phys.: Condens. Matter **19**, 116204 (2007).
[16] See, for example, Fig. 1 of Ref. 3.
[17] S. Paschen, T. Lühmann, S. Wirth, P. Gegenwart, O. Trovarelli, C. Geibel, F. Steglich, P. Coleman, and Q. Si, Nature (London) **413**, 804 (2004).
[18] P. Gegenwart, T. Westerkamp, C. Krellner, Y. Tokiwa, S. Paschen, C. Geibel, F. Steglich, E. Abrahams, and Q. Si, Science **315**, 969 (2007).
[19] O. Trovarelli, C. Geibel, S. Mederle, C. Langhammer, F. M. Grosche, P. Gegenwart, M. Lang, G. Sparn, and F. Steglich, Phys. Rev. Lett. **85**, 626 (2000).
[20] P. Gegenwart, Y. Tokiwa, T. Westerkamp, F. Weickert, J. Custers, J. Ferstl, C. Krellner, C. Geibel, P. Kerschl, K.-H. Müller, and F. Steglich, New J. Phys. **8**, 171 (2006).
[21] P. Gegenwart, Y. Tokiwa, J. Custers, C. Geibel, and F. Steglich, J. Phys. Soc. Jpn. **75**, 155 (2006).
[22] O. Trovarelli, C. Geibel, and F. Steglich, Physica B: Condensed Matter **284-288**, 1507 (2000).
[23] C. M. Varma, P. B. Littlewood, S. Schmitt-Rink, E. Abrahams, and A. E. Ruckenstein, Phys. Rev. Lett. **63**, 1996 (1989).